

Supporting Information

Is Mg-Stabilized Amorphous Calcium Carbonate a Homogeneous Mixture of Amorphous Magnesium Carbonate and Amorphous Calcium Carbonate?

Sheng-Yu Yang,¹ Hsun-Hui Chang,¹ Cang-Jie Lin,¹ Shing-Jong Huang,² and Jerry C. C. Chan^{1*}

¹Department of Chemistry and ²Instrumentation Center, National Taiwan University,
No. 1, Section 4, Roosevelt Road, Taipei 106, Taiwan.

Content

1. Experimental Method
2. Figures
3. Tables
4. References

1. Experimental Method

Sample Preparation and Characterization. ^{13}C -enriched anhydrous Na_2CO_3 (99.5%) was obtained from Cambridge Isotope Laboratories (Andover, USA). All other chemicals were obtained from Acros and used as received, without further purification. Deionized (DI) water was purged with N_2 gas before use. The samples of Mg0.6ACC were prepared as follows. The solution of CaCl_2 (62.5 mM) and MgCl_2 (37.5 mM) was adjusted to the designated pH using aqueous sodium hydroxide (1 M). The ^{13}C -enriched Na_2CO_3 solution (100 mM) was buffered with $\text{NH}_3/\text{NH}_4\text{Cl}$ (1 M) to attain the same pH. The solutions were transferred to two syringes connected to a YSP-101 syringe pump of YMC (Kyoto, Japan). A volume of 5 mL of the $\text{Mg}^{2+}/\text{Ca}^{2+}$ solution was then mixed with 5 mL of the carbonate solution at 4 °C in a YMC microreactor with a volume of 1.2 μL . The flow rate of the reactor was adjusted to 1 mL/min. After discarding the first 0.3 mL of the mixture, the subsequent 8 mL of the mixture was collected in precooled acetone. Precipitates were collected by repeatedly conducting centrifugation (6800 g for 5 min) and washing with precooled ethanol and acetone. The samples were lyophilized and stored in a desiccator. The residual solution mixture (1.7 mL) was collected for pH measurement. The same procedure was repeated with the solution of CaCl_2 (16.7 mM) and MgCl_2 (83.5 mM) for the preparation of the Mg5ACC samples. The samples with isotope enrichment were prepared for the NMR measurements only. All other characterizations were conducted for the natural-abundance samples. Pure ACC and AMC were prepared similarly at pH 8.75 without adding the ammonia buffer.

SEM images were taken on a Hitachi S-4800 field emission scanning electron microscope. The EDX analysis was performed on a LEO 1530 field emission scanning electron microscope equipped with EDX accessories. The ICP-MS

measurements were performed on an Agilent 7500ce system. The standard solutions of 1000 mg/L Ca^{2+} and Mg^{2+} (Merck) were diluted into ppb levels for the calibration measurements.

Solid-State NMR. All SSNMR experiments were carried out at ^{13}C and ^1H frequencies of 100.72 and 400.13 MHz, respectively, on a Bruker Avance III spectrometer equipped with commercial 2.5 mm probe. ^{13}C chemical shift were externally referenced with adamantane as the secondary reference. MAS frequency was 12.5 kHz and the measurement were conducted with sample temperature maintained at 273 K. For ^{13}C direct excitation (Bloch decay) experiments, the recycle delay was set to 120 s. For the $^{13}\text{C}\{^1\text{H}\}$ cross-polarization experiments, the ^1H nutation frequency was set to 50 kHz and that of ^{13}C was ramped linearly through the Hartmann-Hahn matching condition. Two pulse phase modulation (TPPM) proton decoupling of 75 kHz was applied during the acquisition period. The 2D ^{13}C homonuclear correlation was carried out based on proton-driven spin diffusion (PDSD).¹ Quadrature detection in the F1 dimension was accomplished by the States-TPPI approach. For each t_1 increment, 32 scans were accumulated and a total of 128 increments were acquired at steps of 320 μs .

The $^{13}\text{C}\{^1\text{H}\}$ heteronuclear correlation (HETCOR) spectrum was acquired under the conditions of frequency-switched Lee-Goldburg² (FSLG) irradiation during the t_1 evolution to enhance the spectral resolution in the ^1H dimension. The FSLG irradiation was achieved by setting the ^1H decoupling field and the resonance offset at 100 and 70.71 kHz, respectively, so that the effective nutation frequency was equal to 122.5 kHz. The spectrum was acquired at a spin rate of 10 kHz. For each t_1 increment, 256 transients were accumulated and a total of 47 increments were at steps of 75.53 μs .

The spin-diffusion experiments were carried using the pulse sequence shown in Figure S13. The contact time for the CP was set to 0.5 ms to selectively enhance the ^{13}C polarization of the bicarbonate phase. The spin diffusion time, t_{SD} , was varied from 0.1 to 16 s. The spin-diffusion data were analyzed based on the following coupled differential equations:

$$\frac{dI^{\text{HCO}_3^-}}{dt} = -\left(I^{\text{HCO}_3^-} - I_{\text{eq}}^{\text{HCO}_3^-}\right)/\tau_{\text{SD}} + \left(I^{\text{CO}_3^{2-}} - I_{\text{eq}}^{\text{CO}_3^{2-}}\right)/\tau_{\text{SD}}$$

$$\frac{dI^{\text{CO}_3^{2-}}}{dt} = -\left(I^{\text{CO}_3^{2-}} - I_{\text{eq}}^{\text{CO}_3^{2-}}\right)/\tau_{\text{SD}} + \left(I^{\text{HCO}_3^-} - I_{\text{eq}}^{\text{HCO}_3^-}\right)/\tau_{\text{SD}}$$

under the constraint that $I^{\text{HCO}_3^-} + I^{\text{CO}_3^{2-}} = 1$, which essentially requires that each signal must be normalized by the signal sum at the corresponding mixing time. With this procedure, we find that the spin-lattice relaxation times of the two mineral phases, which could be very different, will only affect the quasi-equilibrium distribution of the spin polarizations of the carbonate and the bicarbonate signals but not the τ_{SD} values.³

2. Figures

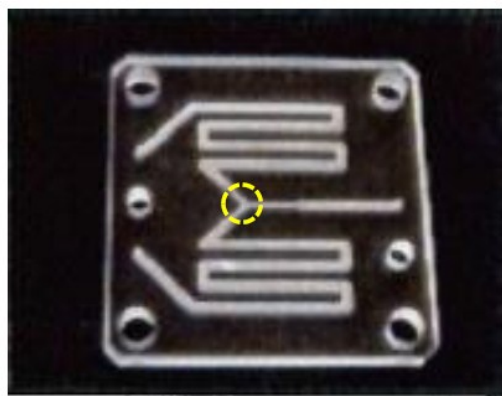


Figure S1. Glass device (KC-M-Y-G, YMC) used for mixing of the stock solutions. The physical size of the device is $30 \times 30 \times 3.2$ mm. The total volume before mixing is $14 \mu\text{L}$ and the mixing chamber (highlighted by the dashed circle) has a volume of $1.2 \mu\text{L}$. The channel has a cross section of 0.5×0.1 mm.

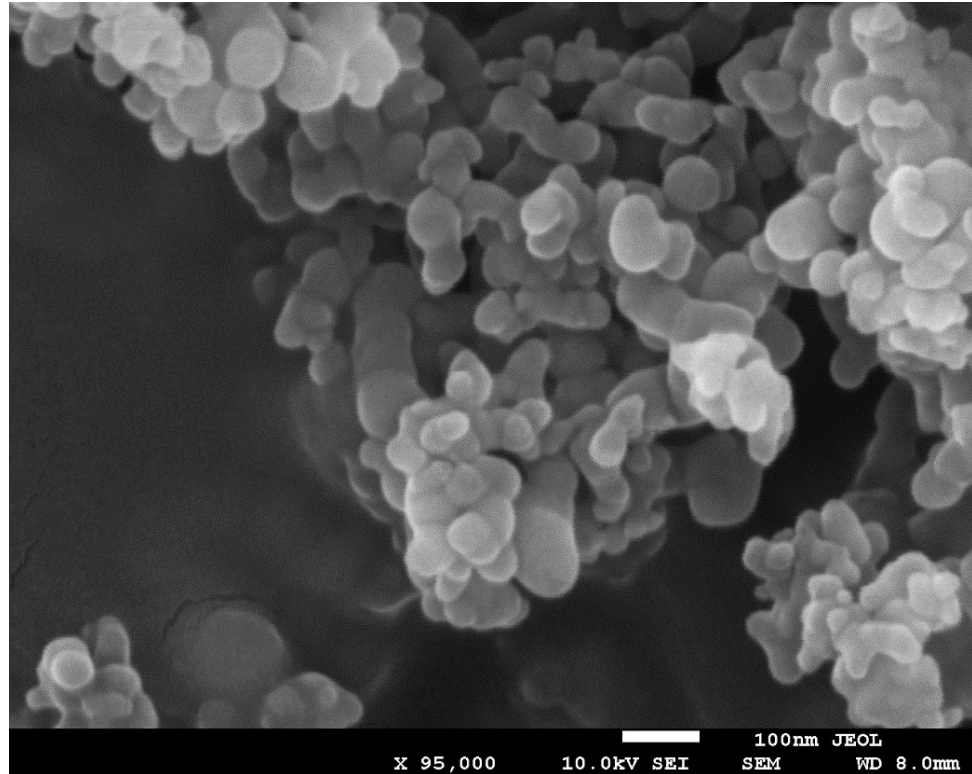


Figure S2. Typical SEM image obtained for MgXACC samples. The mean diameter of the spherical species is in the vicinity of 50 nm.

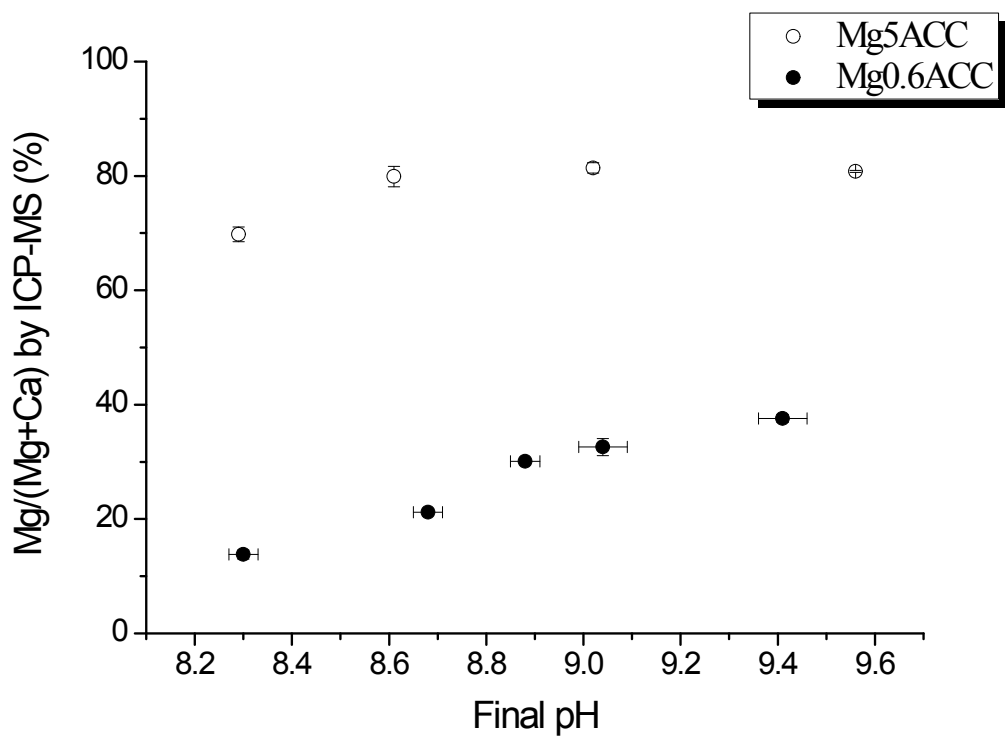


Figure S3.. Mg content of samples Mg5ACC and Mg0.6ACC vs the final pH of the solution mixture.

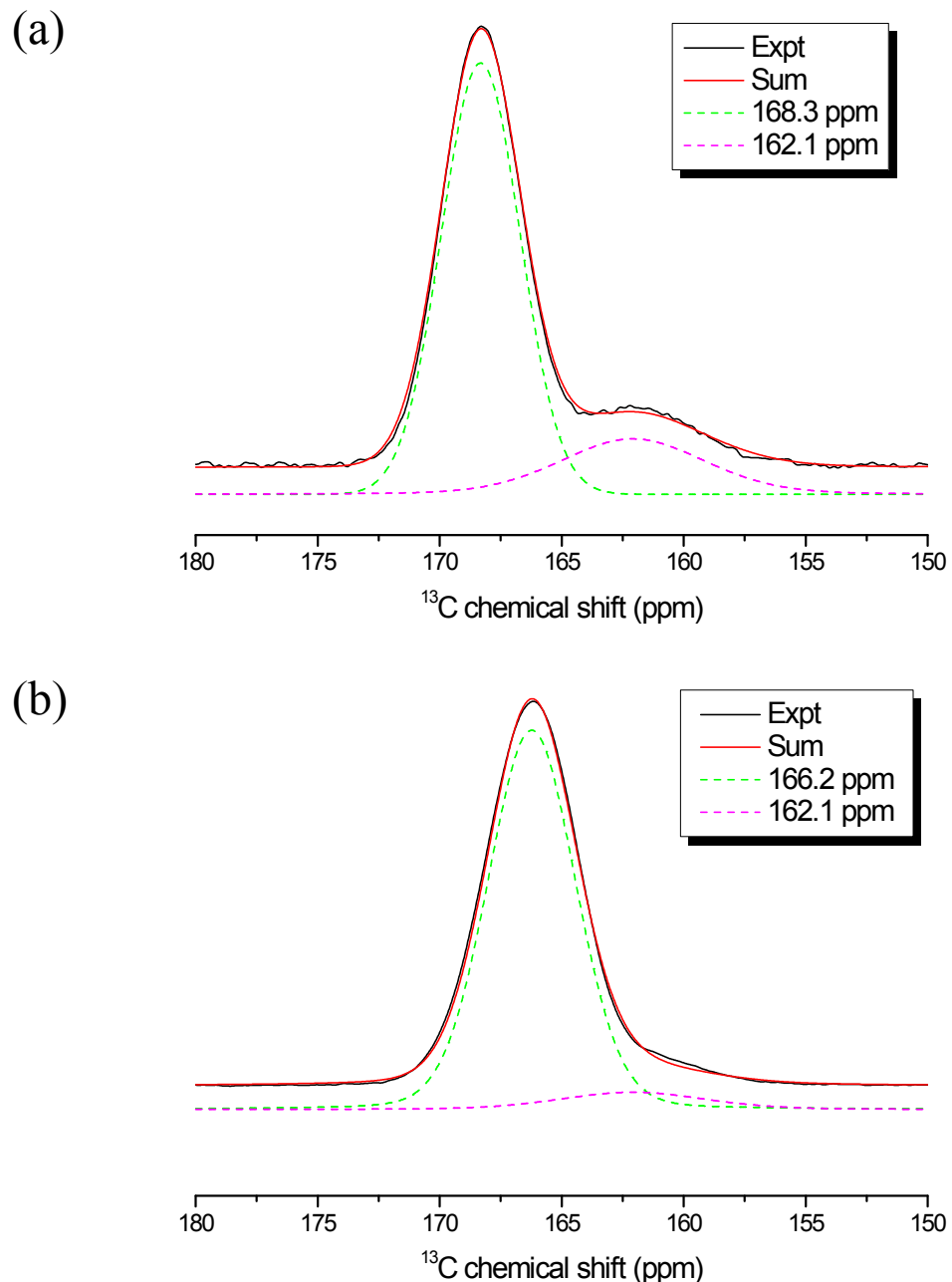


Figure S4. $^{13}\text{C}\{^1\text{H}\}$ CPMAS spectra for (a) pure ACC and (b) **pure** AMC, from which the chemical shifts and line widths of the spectral components at 168.3, 166.2, and 162.1 ppm were determined by deconvolution.

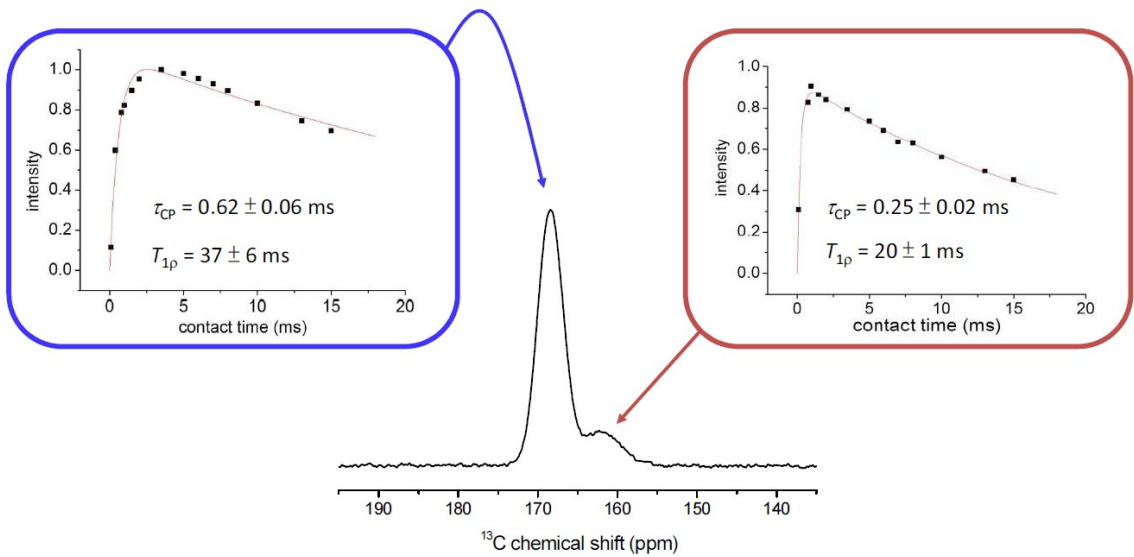


Figure S5. Typical $^{13}\text{C}\{^1\text{H}\}$ variable contact-time CPMAS data obtained for Mg-ACC. The shoulder peak was assigned to HCO_3^- based on its relatively short τ_{CP} (0.25 ms), where the data were analyzed by

$$I(t) = I_0 [1 - \exp(-t/\tau_{\text{CP}})] \exp(-t/T_{1\rho}).$$

Note that the bicarbonate component was not observed for MgXACC prepared at high pH.⁴

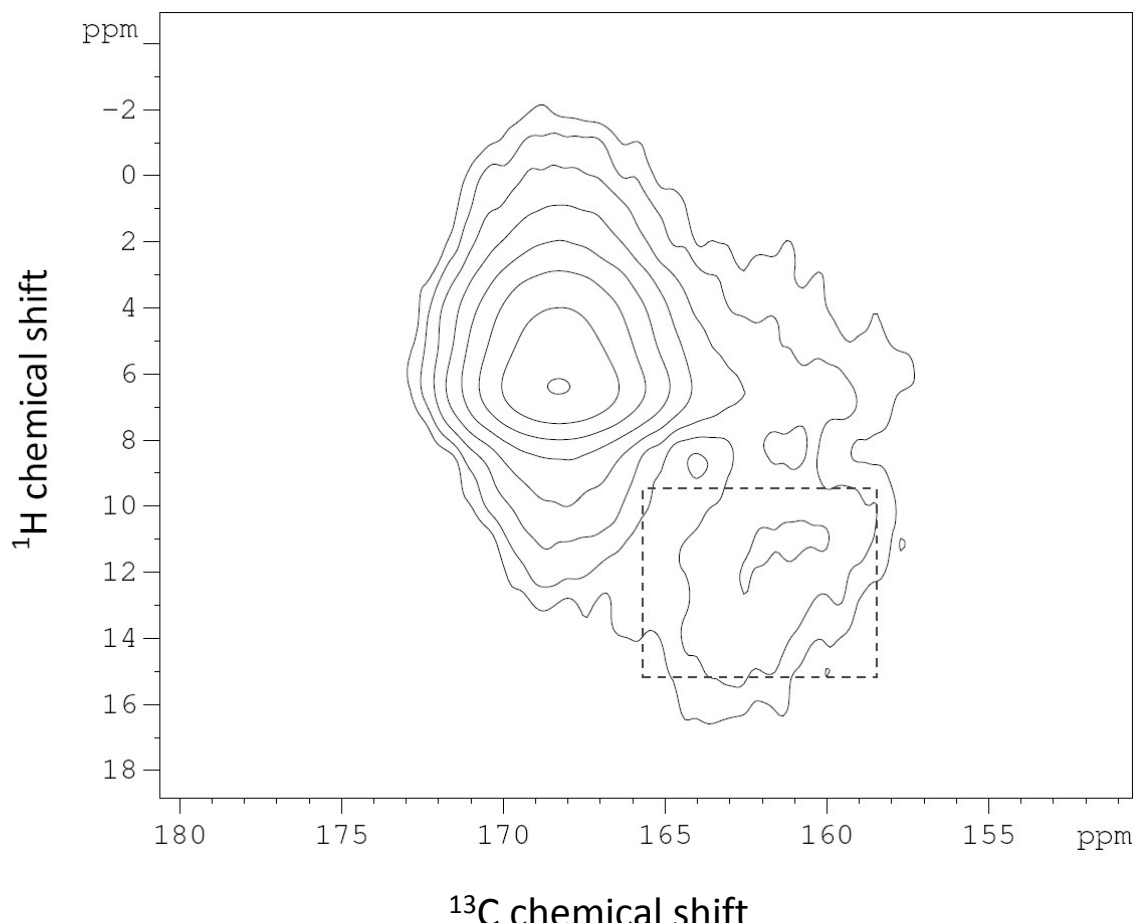


Figure S6. $^{13}\text{C}\{^1\text{H}\}$ FSLG-HETCOR spectrum obtained for Mg0.6ACC prepared at pH 8.30. The correlation peak highlighted by the rectangular dashed region, which centered at 12 and 162 ppm of the ^1H and ^{13}C dimensions, respectively, provided a compelling evidence for the existence of bicarbonate species.⁵ The contour levels were increased by a factor 1.8 successively, where the base levels were set to $3.0 \times$ root-mean-square noise.

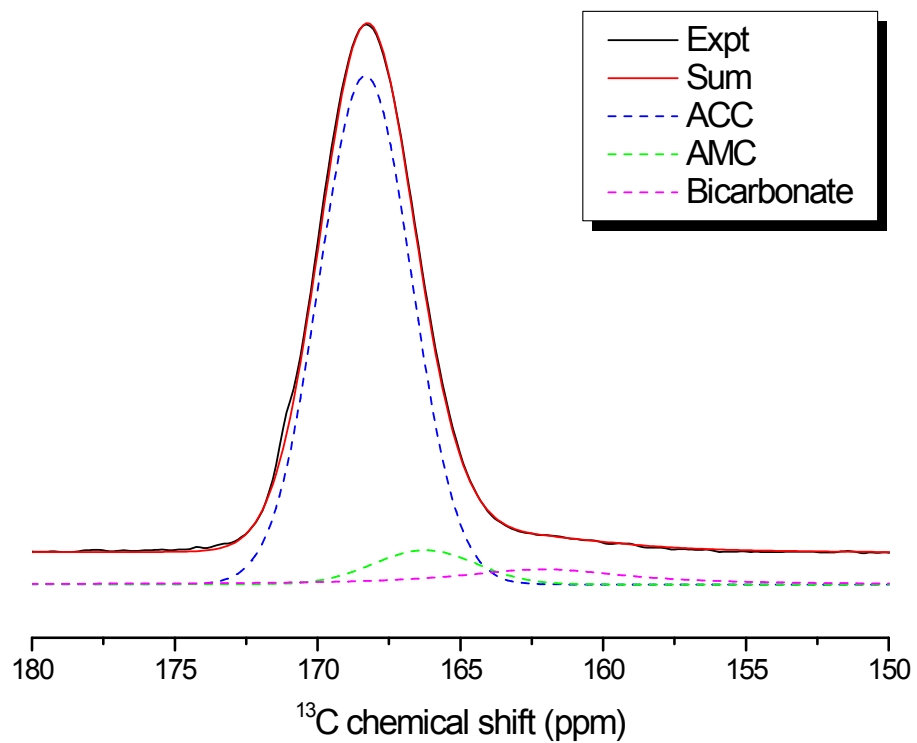
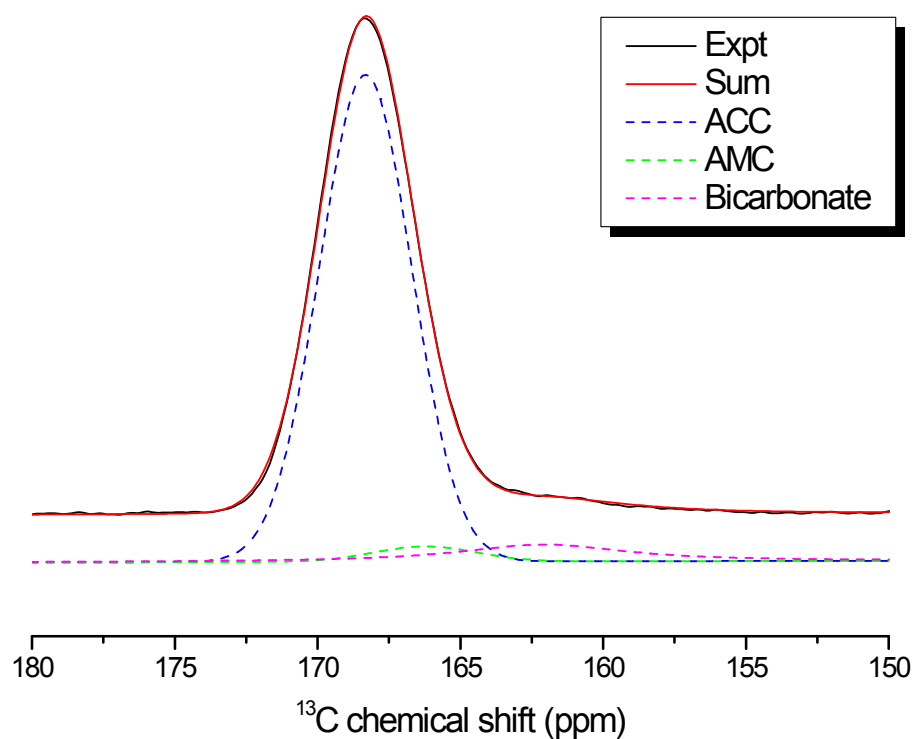


Figure S8. ^{13}C MAS spectrum obtained for Mg0.6ACC prepared at pH 8.68.

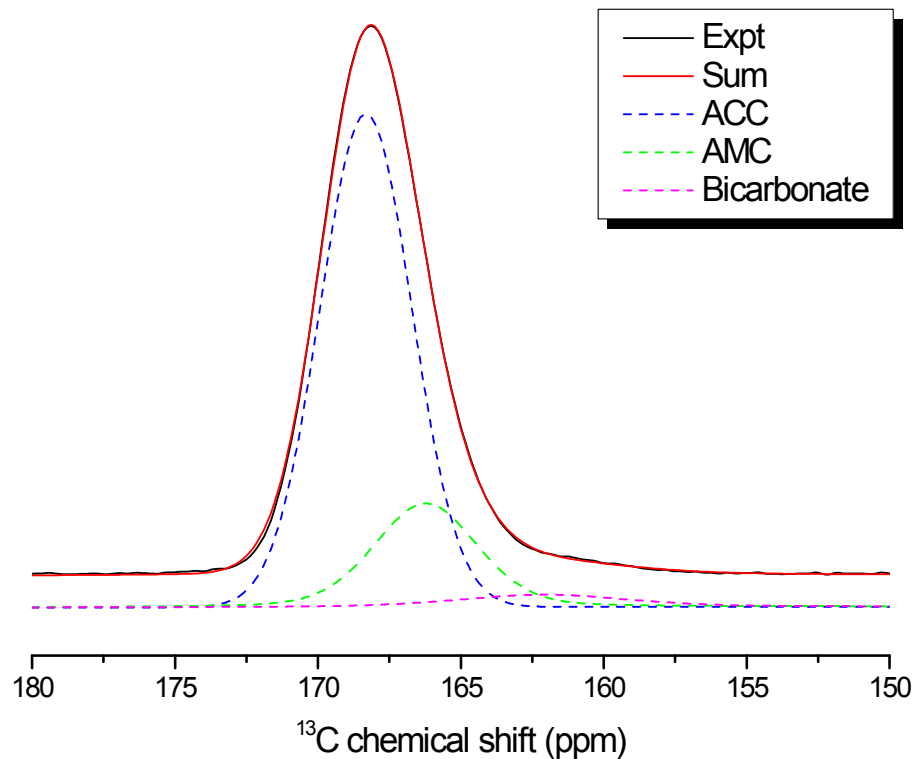


Figure S9. ^{13}C MAS spectrum obtained for Mg0.6ACC prepared at pH 8.88.

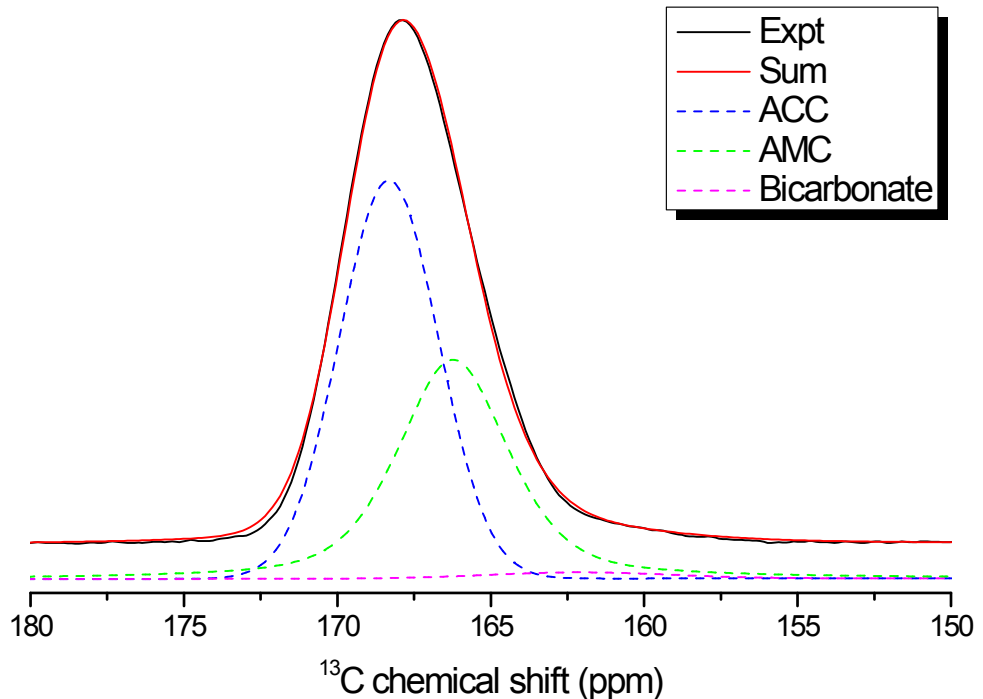
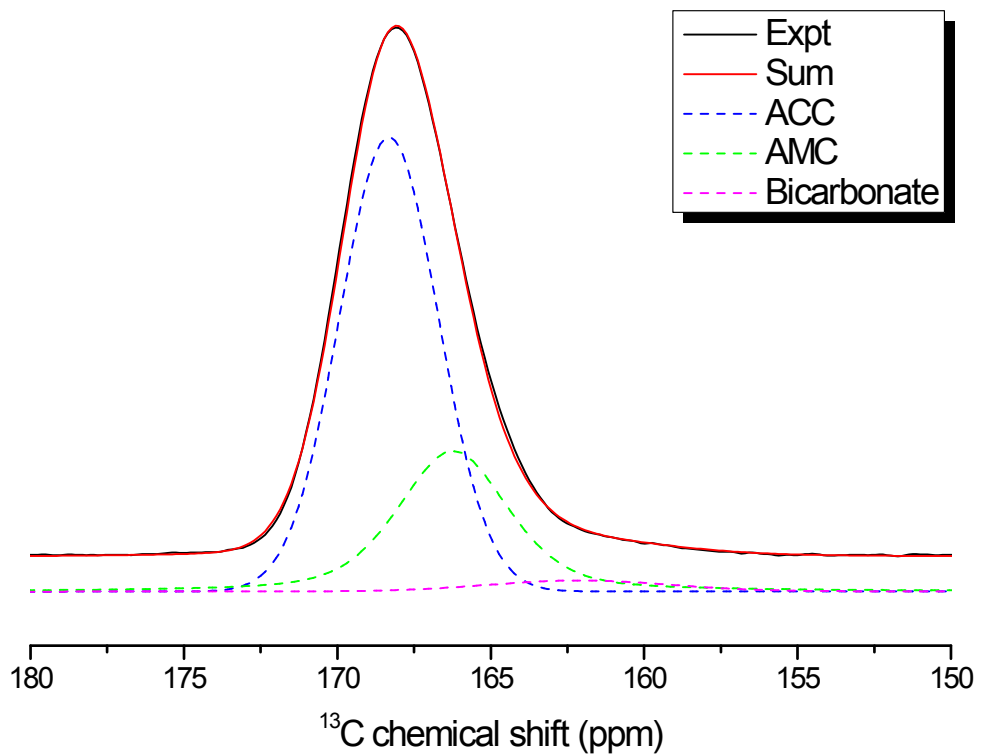


Figure S11. ^{13}C MAS spectrum obtained for Mg0.6ACC prepared at pH

9.41.

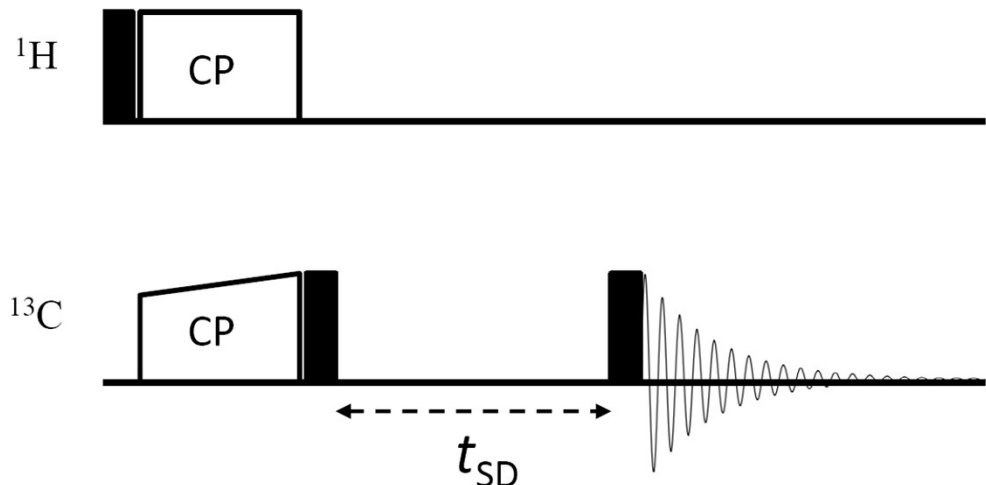


Figure S12. Pulse sequence employed for the spin diffusion experiments.

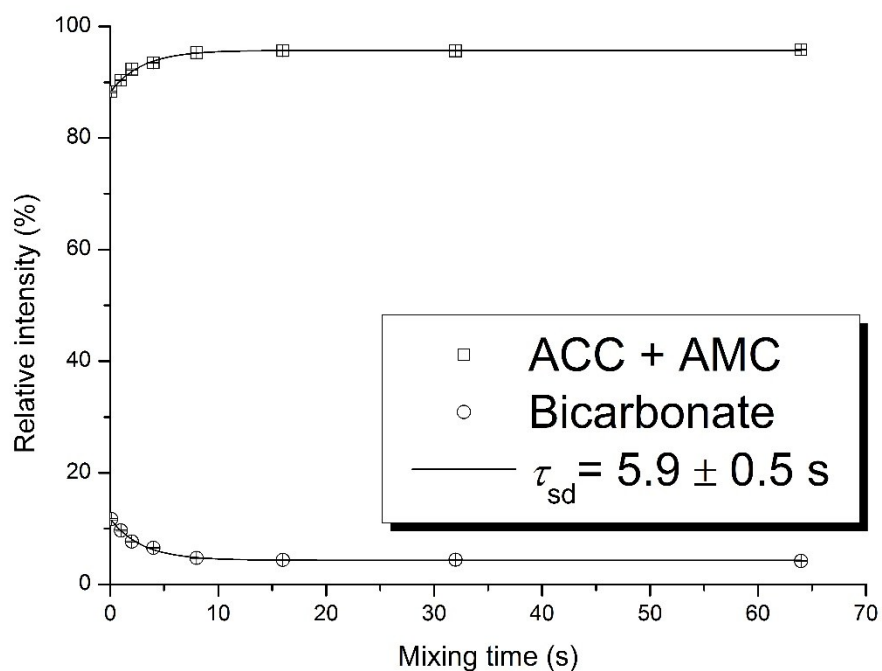


Figure S13. ¹³C spin diffusion results obtained for Mg0.6ACC

prepared at pH 8.30. The data analysis was carried out as described in the experimental section. The error bars are smaller than the symbol size.

3. Tables

Table S1. Summary of the initial pH of the Mg²⁺/Ca²⁺, the final pH after mixing in the micromixer, the Mg content of the MgXACC samples.

Sample	Initial pH ¹	Final pH ¹	Mg content ICP-MS ² (%)	Mg content SEM-EDX ³ (%)
Mg0.6ACC	9.65	9.41 ± 0.05	38 ± 1	36 ± 9
	9.20	9.04 ± 0.05	33 ± 2	31 ± 8
	9.00	8.88 ± 0.03	30 ± 1	28 ± 3
	8.75	8.68 ± 0.03	21 ± 1	21 ± 4
	8.30	8.30 ± 0.03	14 ± 1	13 ± 2
Mg5ACC	9.65	9.56 ± 0.01	80.8 ± 0.2	82 ± 4
	9.20	9.02 ± 0.10	81 ± 1	86 ± 6
	8.75	8.61 ± 0.09	80 ± 2	81 ± 7
	8.30	8.29 ± 0.08	70 ± 1	75 ± 4

¹ All the pH measurements were carried out at room temperature. ² Errors were estimated based on measurements of different samples. ³ Errors were estimated based on measurements at multiple regions.

Table S2. Summary of the TGA data and the chemical composition of selected MgXACC samples.

Samples	Final pH	Weight loss due to bound water	Chemical composition
Mg0.6ACC	9.41 ± 0.05	9.7%	Mg _{0.38} Ca _{0.62} CO ₃ ·0.56H ₂ O
Mg0.6ACC	8.30 ± 0.03	10.6%	Mg _{0.14} Ca _{0.86} CO ₃ ·0.64H ₂ O
Mg5ACC	9.56 ± 0.01	17.9%	Mg _{0.81} Ca _{0.19} CO ₃ ·1.06H ₂ O
Mg5ACC	8.29 ± 0.08	15.1%	Mg _{0.70} Ca _{0.30} CO ₃ ·0.88H ₂ O

4. References

- 1 N. M. Szeverenyi, M. J. Sullivan and G. E. Maciel, *J. Magn. Reson.*, 1982, **47**, 462–475.
- 2 Bielecki, A. C. Kolbert, H. J. M. De Groot, R. G. Griffin and M. H. Levitt, *Adv. Magn. Reson.*, 1990, **14**, 111–124.
- 3 W.-Y. Chen, C.-I. Yang, C.-J. Lin, S.-J. Huang and J. C. C. Chan, *J. Phys. Chem. C*, 2014, **118**, 12022–12027.
- 4 C.-J. Lin, S.-Y. Yang, S.-J. Huang and J. C. C. Chan, *J. Phys. Chem. C*, 2015, **119**, 7225–7233.
- 5 T. W. T. Tsai and J. C. C. Chan, in *Annual Reports on NMR Spectroscopy*, Elsevier, 2011, vol. 73, pp. 1–61.